^{1}H spin–lattice relaxation in water solution of ^{209}Bi counterparts of Gd^{3+} contrast agents

Danuta Kruk, Evrim Umut, Elzbieta Masiewicz, Petr Hermann & Hermann Scharfetter

Published online: 07 Sep 2018.

Submit your article to this journal ⬀

Article views: 627

View related articles ⬀

View Crossmark data ⬀

Citing articles: 3 View citing articles ⬀

Taylor & Francis
Taylor & Francis Group

NMR RELAXOMETRY AND RELATED METHODS

🔓 OPEN ACCESS | Check for updates

^{1}H spin–lattice relaxation in water solution of ^{209}Bi counterparts of Gd^{3+} contrast agents

Danuta Kruk [a], Evrim Umut[a], Elzbieta Masiewicz[a], Petr Hermann [b] and Hermann Scharfetter[c]

[a]Faculty of Mathematics and Computer Science, University of Warmia & Mazury in Olsztyn, Olsztyn, Poland; [b]Department of Inorganic Chemistry, Faculty of Science, Charles University, Prague 2, Czech Republic; [c]Institute of Medical Engineering, Graz University of Technology, Graz, Austria

ABSTRACT

^{1}H spin–lattice relaxation studies of water solutions of Bismuth-ethylenediamine-tetraacetic acid (Bi-EDTA), Bismuth-ethylenediamine-tetrakis(methylenephosphonic) acid (Bi-EDTP), Bismuth-1,4,7,10-tetraazacyclododecane-1,4,7,10-tetraacetic acid (Bi-DOTA), Bismuth-1,4,7,10-tetraazacyclodo decane-1,4,7,10-tetrakis(methylenephosphonic acid) (Bi-DOTP) and Bismuth-1,4,7,10-tetraazacyclo dodecane-1,4,7-triacetic acid (Bi-DO3A) have been performed in order to compare Quadrupole Relaxation Enhancement (QRE) effects with Paramagnetic Relaxation Enhancement (PRE) from the perspective of exploiting the first one as a novel contrast mechanism for Magnetic Resonance Imaging (MRI). The selected compounds can be considered as ^{209}Bi counterparts of Gd^{3+} complexes. The relaxation experiments have been performed in a broad frequency range of 5 kHz–30 MHz. The relaxation contribution associated with QRE has been extracted from the data and compared with PRE. Similarities and differences between the two effects have been discussed.
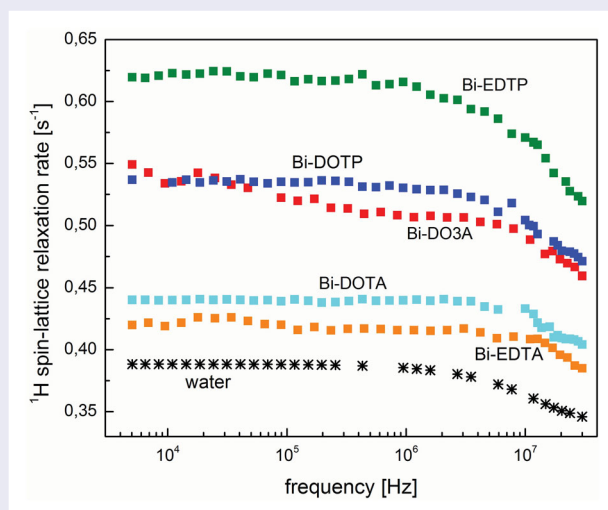
Introduction

Magnetic Resonance Imaging (MRI) is the most versatile tool for medical diagnostics. Nevertheless, to increase the difference (contrast) between ^{1}H relaxation in healthy and pathological tissues, contrast agents are needed [1,2]. Currently, the contrast is achieved by exploiting Paramagnetic Relaxation Enhancement (PRE) effects [3,4]. Paramagnetic contrast agents include lanthanide complexes (often Gd^{3+}), for instance: Gd-DOTA (Dotarem® or Clariscan®, Guerbet group), Gd-DTPA (Magnevist®, Bayer Pharma) or GdHP-DO3A (ProHance, Bracco Diagnostics) [5,6]. The enhancement of ^{1}H relaxation originates from strong dipole–dipole interactions between proton and electron spins. One can distinguish inner-sphere and outer-sphere PRE. In the first case, water molecules form a coordination sphere

around the contrast agent molecule and the whole species undergoes rotational dynamics – in consequence, the proton spin – electron spin dipole–dipole interaction fluctuates in time due to molecular tumbling. In the case of outer-sphere, PRE water molecules do not stay in a bound position (a coordination sphere) – this implies that the dipole–dipole coupling is modulated by relative translational diffusion of the paramagnetic molecule and water molecules. The scenario is completed by water exchange between the coordination sphere (if present) and bulk [7,8]. As the electron gyromagnetic factor is 659 times larger than the proton gyromagnetic factor and, moreover, the relaxation rate depends on the square of the spin quantum number, one can expect very large PRE values. In fact, the relaxation rate is very considerably reduced by electron spin relaxation caused by Zero-Field Splitting interactions [9–14].

The electron spin relaxation acts as an additional source of modulations of the proton spin – electron spin dipole–dipole coupling.

Recently an entirely new concept of obtaining contrast in MRI has been proposed by some of us [15,16]. The concept is based on Quadrupole Relaxation Enhancement (QRE) caused by dipole–dipole couplings between protons (more general – spin 1/2 nuclei) and nuclei possessing a quadrupole moment (referred to as quadrupole nuclei). Considering analogies between PRE and QRE one can point out two of them: the first one is the analogous scenario of interactions of water (solvent) protons with species carrying a quadrupole nucleus (instead of a paramagnetic ion), while the second one is the corresponding Hamiltonian formalism of ZFS and quadrupole couplings [17]. As far as differences are concerned, there are many of them. Let us first consider the case of slow molecular tumbling in comparison to slowly rotating paramagnetic systems. When the rotational dynamics is slow (much slower than relaxation processes in the system), the energy level structure of the quadrupole nucleus is determined by a superposition of its quadrupole and Zeeman interactions (the orientation of the principal axis system of the electric field gradient tensor with respect to the direction of the external magnetic field is fixed – i.e. time-independent) [18,19]. In consequence, there are magnetic fields at which the ^{1}H Zeeman splitting (resonance frequency) matches one of the transition frequencies of the quadrupole nucleus between its energy levels. At such magnetic fields the ^{1}H polarisation can be taken over by the quadrupole nucleus that manifests itself as an enhancement of the ^{1}H spin–lattice relaxation (increasing of the relaxation rate), referred to as quadrupole peaks [20–31].

This means that QRE is a frequency-specific effect, in contrary to PRE that is always present because of the strong dipole–dipole coupling. This is considered as a great advantage of potential contrast agents based on QRE as subtle changes in the electric field gradient in pathological tissues would lead to switching on and off of the contrast effect [15,16]. For slow molecular tumbling one also observes a relaxation maximum (on the top of the overall PRE). It comes from frequency dependencies of electron spin relaxation rates; it is obvious that for paramagnetic systems one cannot expect to match the ^{1}H resonance frequency with electron spin transitions determined by ZFS and electron Zeeman interactions. The PRE maximum is broad and single, while QRE peaks are narrow and their number depends on the spin quantum number. In the case of fast rotation PRE and QRE effects are more similar. The energy level structure of both: the electron spin and spin of the quadrupole nucleus is fully determined by their Zeeman interactions. Due to the Zeeman energy structure, there are no relaxation maxima (neither for PRE nor QRE). The ZFS and quadrupole interactions act as a relaxation mechanism for the electron and nuclear (quadrupole) spin, respectively. Moreover, in both cases the relaxation is slower than the rotational dynamics and, in consequence, it can be neglected.

In this work, we discuss QRE effects for ^{209}Bi counterparts of well-known Gd^{3+} complexes being in use as paramagnetic contrast agents: Bismuth-ethylenediamine-tetraacetic acid (Bi-EDTA), Bismuth-ethylenediamine-tetrakis(methylenephosphonic) acid (Bi-EDTP), Bismuth-1,4,7,10-tetraazacyclododecane-1,4,7,10-tetraacetic acid (Bi-DOTA), Bismuth-1,4,7,10-tetraazacyclododecane-1,4,7,10-tetrakis(methylenephosphonic acid) (Bi-DOTP) and Bismuth-1,4,7,10-tetraazacyclododecane-1,4,7-triacetic acid (Bi-DO3A). The molecules undergo fast rotation due to their size and low viscosity of water. The purpose of the studies is to recognise to which extent the PRE and QRE processes are analogous and get a better awareness of possible difficulties which one can face when attempting to exploit QRE as a contrast mechanism.

Theory

The description of ^{1}H spin–lattice relaxation induced by dipole–dipole interactions with quadrupole nuclei depends on the time scale of dynamical processes modulating spin interactions. As in this work, we consider relaxation in water solutions of relatively small molecules, one can expect a fast molecular tumbling. This implies fast fluctuations of the orientation of the principal axis system of the electric field gradient at the position of the quadrupole nucleus with respect to the direction of the external magnetic field. In consequence, the

quadrupole interaction does not contribute to the energy level structure of the quadrupole nucleus (that is entirely determined by its Zeeman coupling) and the theoretical description greatly simplifies. The expression for ^{1}H spin–lattice relaxation rate, $R_1(\omega_I)$ (ω_I denotes the ^{1}H resonance frequency) is given in the following [31–33]:

$$R_1(\omega_I) = \frac{2}{15}\left(\frac{\mu_0}{4\pi}\frac{\gamma_I\gamma_S\hbar}{r^3}\right)^2 S(S+1)$$
$$\times \left[J(\omega_I - \omega_S) + 3J(\omega_I) + 6J(\omega_I + \omega_S)\right] \quad (1)$$

where ω_S, γ_S and S denote the resonance frequency of the quadrupole nucleus, its gyromagnetic factor and spin, respectively, the proton gyromagnetic factor is denoted as γ_I, while r is the inter-spin distance [32]. In Equation 1 it has been assumed that the relaxation is of inner-sphere origin. This means that water molecules form a coordination sphere around the compound molecule and the whole species rotate until the water molecule gets replaced by another one. In such a case, the spectral density $J(\omega)$ is given in the following [31–33]:

$$J(\omega) = \frac{\tau_c}{1 + \omega^2\tau_c^2} \quad (2)$$

The correlation time, τ_c, reflects the two sources of modulations of the $I - S$ dipole–dipole coupling, namely the molecular tumbling and the quadrupole spin relaxation [33,34]. As in this case, one can safely assume that the rotational dynamics is much faster than the quadrupole relaxation, one can neglect the second contribution and set: $\tau_c = \tau_{rot}$, where τ_{rot} denotes the rotational correlation time. In analogy to paramagnetic systems, the ^{1}H spin–lattice relaxation rate, $\tilde{R}_1$, obtained as a difference between the relaxation rate measured for the solution and pure water relaxation rate at the corresponding frequency, depends on the concentration of molecules carrying the quadrupole nucleus and the coordination number (the number of bound water molecules) as:

$$\tilde{R}_1(\omega_I) = \frac{Pq}{R_1^{-1}(\omega_I) + \tau_{ex}} \quad (3)$$

where q is the coordination number, while P denotes the mole fraction of water protons in the bound position [35]. Equation (2) includes the exchange lifetime, τ_{ex}, describing how long water molecules stay in the inner-sphere (bound position). For the case of fast rotation, one can expect a small value of the relaxation rate $R_1(\omega_I)$ (the relaxation is slow). In consequence, very likely the relaxation time is much longer than the exchange lifetime and the last quantity can be neglected in Equation (2). Thus, knowing the P and q values, the measured ^{1}H spin–lattice relaxation rate, $\tilde{R}_1$, depends only on two parameters: r and τ_{rot}.

Experimental details

^{1}H NMR spin–lattice relaxation measurements were performed on aqueous solutions of five ^{209}Bi containing complexes: Bi-DOTA, Bi-DOTP, BiDO3A, Bi-EDTA and Bi-EDTP. The structures of the complexes are shown in Figure 1. The measurements were performed at 295 K in the frequency range of 5 kHz–30 MHz using a Stelar Spinmaster FFC relaxometer. The concentration of the solutions was 0.15 M. Moreover, to demonstrate the linear dependence of $\tilde{R}_1(\omega_I)$ on the concentration, additional relaxation measurement on 0.3M Bi-EDTA complex solution was also performed. In all cases, the relaxation can be described by a single-exponential. Examples of the ^{1}H magnetisation curves recorded vs. time are shown in Figure 2. As a reference, ^{1}H spin–lattice relaxation dispersion profile of water at 295 K was also collected.

The compounds were synthesised by complexation reaction of Bi(NO$_3$)$_3$·5H$_2$O with appropriate ligand in 0.95:1 molar ratio in water. The Bi(NO$_3$)$_3$ and anhydrous ethylenediamine-tetraacetic acid (EDTA) were purchased from commercial suppliers. The 1,4,7,10-tetraazacyclododecane-1,4,7,10-tetraacetic acid hydrate, DOTA·4H$_2$O [36], 1,4,7,10-tetraazacyclododecane-1,4, 7,10-tetrakis(methylenephosphonic acid), DOTP [37], and diammonium salt of ethylenediamine-tetrakis (met hylenephosphonic acid), (NH$_4^)$$_2$(EDTP)·H$_2$O [38], were obtained by published procedure. The DO3A was obtained by hydrolysis of its t-butyl ester [39] in trifluoroacetic acid / CH$_2$Cl$_2$ and was used in the complex synthesis immediately without isolation.

The powdered ligand (DOTA·4H$_2$O / DOTP / DO3A / EDTA / (NH$_4$)$_2$(EDTP)·H$_2$O; 600 mg) or, DO3A obtained from the corresponding molar amount of tBu$_3$DO3A, was dissolved in deionised water (20 mL) and the solution pH was adjusted with aq. NaOH (5%) to pH ∼6. The corresponding molar amount of Bi(NO$_3$)$_3$·5H$_2$O was dissolved first in concentrated (65%) aq. nitric acid (2 mL) and, after evaporation of the solution almost to the dryness, the residual solution was diluted by 15% aq. nitric acid. Thereafter, the acidic Bi(NO$_3$)$_3$ solution was portion-wise (approx. 0.2 mL) added to the aqueous solutions of the ligands at 60°C under magnetic stirring. During mixing, the added portion of Bi(III) precipitated as hydroxide and it was quickly dissolved. Then, pH of the solutions was re-adjusted with the aq. NaOH back to pH ∼6–7. Then, next portion of the Bi(III) solution was added. The pH balance is necessary – when the solutions of the ligands become too acidic (pH < 3), the water solubility of the ligands/complexes decreases due to protonation of the carboxylate or phosphonate groups in the ligands. Whereas
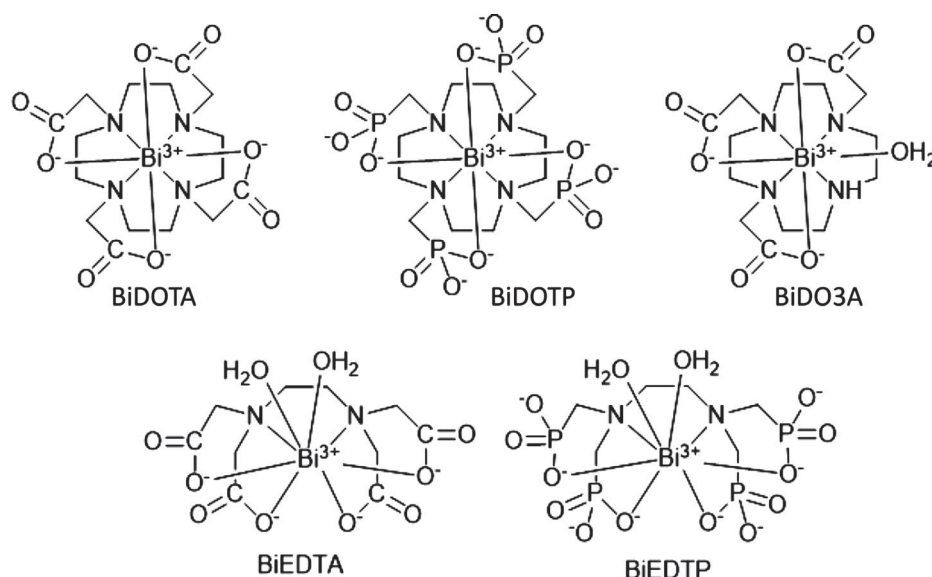
Figure 1. Structure of [209]Bi compounds: 1,4,7,10-tetraazacyclododecane-1,4,7,10-tetraacetic acid (DOTA), 1,4,7,10-tetraazacyclododecane-1,4,7,10-tetrakis(methylenephosphonic acid) (DOTP), 1,4,7,10-tetraazacyclododecane-1,4,7-triacetic acid (DO3A), ethylenediamine-tetraacetic acid (EDTA), ethylenediamine-tetrakis(methylenephosphonic acid) (EDTP). (Structures of the fully deprotonated complexes are shown).

very high alkaline pH (pH > 11) promotes the formation of polymeric Bi(OH)$_3$ instead of complexation with the ligands. In the case of complexes with the macrocyclic ligands, Bi-DOTA, Bi-DOTP and Bi-DO3A, the final solutions were left in oil bath at 60°C under stirring for more than 12 h (i.e. overnight) to ensure the complete formation of the *in-cage* complexes where all donor atoms are coordinated and the Bi(III) ion is bound inside the ligand cavity. Precipitation of the [209]Bi complexes from the solutions was carried by a careful acidification of the solutions to pH $\sim$ 3 by 15% aq. nitric acid followed by a slow addition of ethanol and/or acetone. The microcrystalline solids, i.e. Na[Bi(DOTA)] [40], Na[Bi(H$_4$DOTP)], [41], [Bi(DO3A)], Na[Bi(EDTA)] and Na[Bi(H$_4$EDTP)]) were then filtered through a frit (medium porosity), washed with ethanol and acetone, and finally left to dry on air at room temperature overnight. The Bi-DOTA, Bi-DO3A and Bi-EDTA complexes exhibits a high solubility in water at neutral pH, whereas the Bi-DOTP and Bi-EDTP complexes are only soluble in water at pH > 9–10. Accordingly, the measured solutions were adjusted by diluted aq. NaOH to pH 7 or 9.5, respectively.

Results and analysis

[1]H spin–lattice relaxation dispersion profiles for 0.15 M water solutions of Bi-DOTA, BiDO3A, Bi-EDTA, Bi-DOTP and Bi-EDTP at 295 K are shown in Figure 3(a). The figure also includes ^{1}H spin–lattice relaxation data for pure water for comparison. Figure 3(b) shows

$\tilde{R}_1$ values obtained as a difference between the relaxation rates shown in Figure 3(a) and water relaxation. Comparing the low frequency value of the relaxation rates, $\tilde{R}_1$, that are given as: $\tilde{R}_1(\omega_I \to 0) = \tilde{R}_{10} = C_{DD}\tau_{rot}$(the symbol C_{DD} refers to a dipolar relaxation constant), where $C_{DD} = 33Pq\left(\frac{\mu_0}{4\pi}\frac{\gamma_I\gamma_S\hbar}{r^3}\right)^2$(for $S = 9/2$) and $C_{DD} = \frac{8}{3}Pq\left(\frac{\mu_0}{4\pi}\frac{\gamma_I\gamma_S\hbar}{r^3}\right)^2$(for $S = 1$) one can conclude that the decreasing of the relaxation rates (Bi-EDTP, Bi-DOTP, Bi-DO3A, Bi-DOTA, Bi-EDTA) correspond, in good approximation to the decreasing size of the molecules. This is a reasonable result taking into account that one can expect a faster rotation (smaller τ_{rot}values) for small molecules. Figure 3(a) (and hence Figure 3(b)) clearly shows that the presence of the [209]Bi containing molecules enhances the relaxation of water protons. At this stage one should note that the contribution of the intrinsic protons of the [209]Bi containing molecules to the overall pool of protons in the system is on the level of 2.7% (EDTP), 4.3% (DOTP), 3.1% (DO3A), 3.8% (DOTA) and 2.2% (EDTA). The low amount of the intrinsic protons implies that the detected ^{1}H magnetisation stems from water (solvent) protons. The visible enhancement of the water protons relaxation confirms that the exchange lifetime does not dominate the denominator in Equation (3). Explicitly, this means that the exchange lifetime is shorter than the relaxation time R_1^{-1}; actually, this condition is not difficult to fulfil for QRE as in this case the relaxation time $R_1^{-1}$is long in contrary to paramagnetic systems. In Figure 4, it has been demonstrated that the relaxation
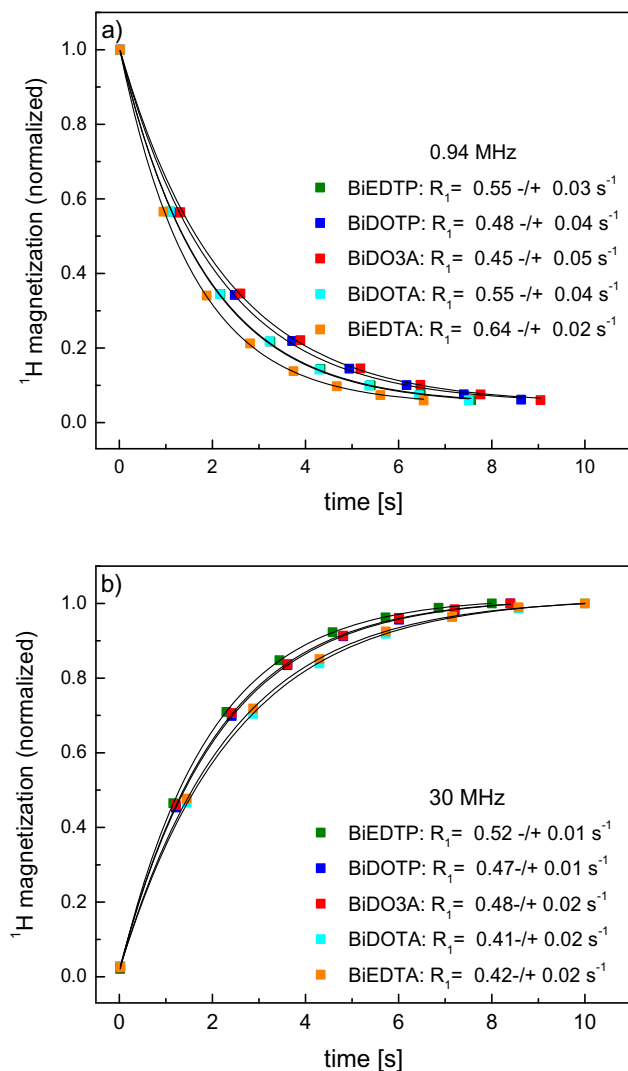
Figure 2. ^{1}H magnetisation curves versus time for 0.15 M water solutions of compounds listed in the figure collected at (a) 0.94 MHz, (b) 30 MHz at 295 K.

Figure 3. (a) ^{1}H spin-lattice NMRD data for 0.15 M water solution of ^{209}Bi containing EDTP, DOTP, DO3A, DOTA, EDTA, and water at 295 K; (b) differences between the relaxation rates shown in (a) and water relaxation rates. The experimental error in (a) does not exceed 5%. Solid lines – fits according to Equation (4).

rate, $\tilde{R}_1$, is indeed proportional to the concentration of the compounds, using Bi-EDTA as an example.

Taking into account that $\omega_S << \omega_I$, one can simplify Equations (1–3) to the form:

$$\tilde{R}_1(\omega_I) = C_{DD} \frac{\tau_{rot}}{1 + \omega_I^2 \tau_{rot}^2} \qquad (4)$$

that has been used to reproduce the relaxation dispersion profiles for Bi-EDTP and Bi-DOTP (solid lines in Figure 3(b)). The obtained values yield: $C_{DD} = 4.81 * 10^6 Hz^2$, $\tau_{rot} = 13.3$ ns (Bi-EDTP) and $C_{DD} = 3.05 * 10^6 Hz^2$, $\tau_{rot} = 9.35$ ns (Bi-DOTP). The relatively long correlation times indicate clustering effects. The relaxation dispersion profiles for these two compounds do not exhibit any QRE features. In this context it is worth to stress that ^{1}H spin–lattice relaxation profiles for the corresponding solids (Figure 5) do not show any QRE
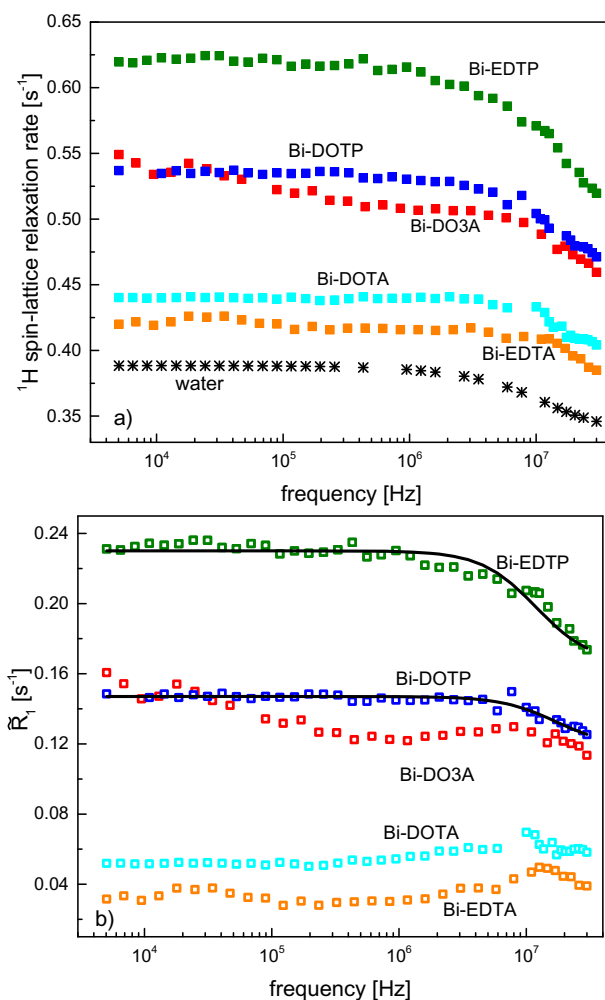
peaks neither associated with ^{14}N nor ^{209}Bi. Actually, as far as ^{1}H spin–lattice relaxation experiments for solids are concerned, the measurements were possible only for Bi-EDTP and Bi-DOTP; the other compounds in solid presumably exhibit to short spin–spin relaxation to detect the signal. The analysis of the Bi-DOTP data should be treated with caution as DOTP is considered as an outer-sphere compound [6]. As already explained in the introduction, this means that $q = 0$, i.e. the dipole–dipole coupling between the paramagnetic (quadrupole) centre and the water protons is modulated by translational diffusion of the species involved. However, as the relaxation dispersion (Figure 3(a,b)) does not show much-pronounced features, it is hard to consider different motional models in this case.

Analogous analysis for water solution of Bi-DO3A is problematic for two reasons. The first one is the
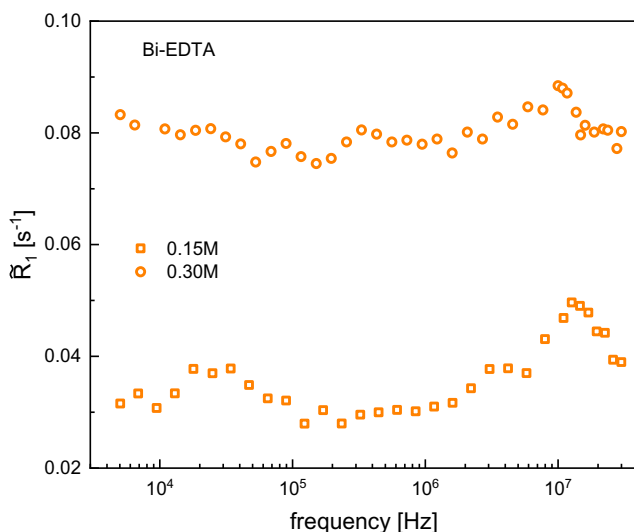
Figure 4. ¹H spin-lattice NMRD data for 0.15 and 0.3 M water solution of ²⁰⁹Bi containing EDTA at 295 K; the ratio between the relaxation rates is about 2 as expected from the concentration.
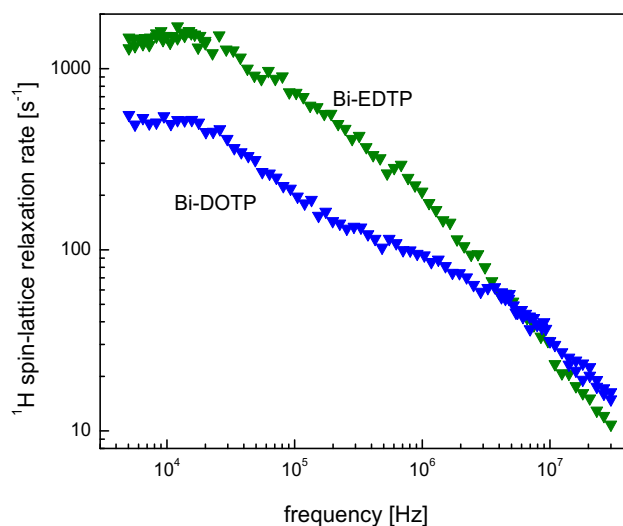

Figure 5. ¹H spin-lattice NMRD data of ²⁰⁹Bi containing EDTP and DOTP in solid state at 295 K.

relaxation dispersion at low frequencies that likely stems from molecular aggregation. The presence of clusters implies a distribution of rotational correlation times corresponding to the distribution of cluster sizes and, in consequence, a dispersion of relaxation as the rotational correlation times are longer than for a single molecule. The second reason is a slight peak around 10 MHz. It is so weak that one can attribute them to experimental uncertainties, but anyway because of its presence, one can hardly reproduce the relaxation profile in terms of Equation (4). PRE for Gd-DO3A in water solution has been investigated in [42]. Analysis of the data (at 298 K) has provided $\tau_{rot} = 66 ps$ and $r = 3.15 Å$. Taking into account that for this compound $q = 2$, one can resolve

whether the $\tilde{R}_1$ relaxation contribution stems from ¹H-¹⁴N or ¹H-²⁰⁹Bi dipole–dipole couplings by analysing the value of C_{DD} that leads to an agreement with the data shown in Figure 3(a,b). The values of $Pq\left(\frac{\mu_0}{4\pi}\frac{\gamma_I\gamma_S\hbar}{r^3}\right)^2$ for ¹⁴N and ²⁰⁹Bi yield: $16.11 * 10^3 \, Hz^2$ and $79.7 * 10^3 \, Hz^2$, respectively. As $P = c/55.6$, where c denotes concentration of the solute molecules (in mole) one obtains in the low frequency range $\tilde{R}_1 = 2.84 * 10^{-6} \, s^{-1}$ (for ¹⁴N) and $\tilde{R}_1 = 1.74 * 10^{-4} \, s^{-1}$ (for ²⁰⁹Bi), for $c = 0.15$ M. The comparison with the experimental value $(\tilde{R}_1 = 6.47 * 10^{-4}$ $s^{-1})$ leads to the conclusion that the QRE is, in this case, dominated by the ¹H-²⁰⁹Bi dipole–dipole relaxation pathway.

Neglecting experimental uncertainties (the experiment poses difficulties due to slow relaxation) one can say that the ¹H spin–lattice relaxation profile for Bi-DOTA solution is flat. It is however of interest to compare the QRE with PRE for water solution of Gd-DOTA. The relaxivity ($\tilde{R}_1$ referred to 1mM concentration) for water solution of Gd-DOTA at 295 K in the low-frequency range yields: $11.8 \, mM^{-1} s^{-1}$, while the exchange lifetime yields: $\tau_{ex} = 244ns$ and $q = 1$ [43]. Knowing the parameters one can extract from Equation (4), the R_1 value for Gd-DOTA and compare it with R_1 for Bi-DOTA (referring to the same concentration of 1mM); one obtains: $x = R_1^{Gd}/R_1^{Bi} = 3.6 * 10^4$. Taking into account that electron spin of Gd³⁺ is 7/2, the expected ratio, neglecting the electron spin relaxation, is given as: $x = \frac{63}{4S(S+1)}\left(\frac{\gamma_e}{\gamma_S}\right)^2$, where γ_e denotes electron gyromagnetic factor. Thus, the expected ratio yields $x = 6.52 * 10^8$ (for ¹⁴N) and $x = 1.07 * 10^7$ (for ²⁰⁹Bi) and is much higher than the experimental one that is: $3.6 * 10^4$ (referring to 1 mM concentration of Bi-DOTA in water). This shows to which extent the electron spin relaxation reduces the PRE. The rotational correlation time for Gd-DOTA has been estimated as 77 ps (298 K), while the inter-spin distance as 3.13 Å [43]. Substituting the values into Equation (4) and comparing the result with experiment one can again confirm that the $\tilde{R}_1$ contribution shown in Figure 3(b) stems from ¹H-²⁰⁹Bi dipole–dipole interactions. Eventually, we turn attention to the Bi-EDTA relaxation dispersion profiles (Figures 3(b) and 4). Surprisingly, the data show effects that one can interpret as some QRE peaks. One should note that this effect is not visible in Figure 3(a); it only divulges after extracting the relaxation contribution originating from pure water. At this stage we wish to stress again that the experiment is difficult because of very slow relaxation and the uncertainty accumulates when taking a difference between the data shown in Figure 3(a) and water relaxation rates. Nevertheless, the peak is quite well pronounced and its

presence can only be attributed to large clusters – otherwise the rotational dynamics is too fast. Nevertheless, this example shows that for Bi-EDTA incorporated into nanoparticles to slow down rotational dynamics one can expect at higher frequencies QRE effects associated with ^{209}Bi and this pathway should be explored.

Conclusions

^{1}H spin–lattice relaxation profiles for water solution of Bi-EDTP, Bi-DOTP, Bi-DO3A, Bi-DOTA, Bi-EDTA have been decomposed into a contribution associated with the solvent (water) ^{1}H-^{1}H dipole–dipole interactions and a component originating from ^{1}H-^{209}Bi dipole–dipole interactions (QRE contribution). The magnitude of the last contribution corresponds to the parameters (the rotational correlation time and the inter-spin distance) obtained from an analysis of PRE effects for the analogous Gd^{3+} compounds. For Bi-EDTA quadrupole peaks have been observed. This finding indicates that by slowing down the rotational motion (for instance by incorporating the compound into a nanoparticle) one should be able to obtain sharper and better-pronounced quadrupole peaks that are of interest for MRI contrast agents based on the QRE.

Acknowledgements

Disclosure statement

No potential conflict of interest was reported by the authors.

Funding

ORCID

Danuta Kruk http://orcid.org/0000-0003-3083-9395
Petr Hermann http://orcid.org/0000-0001-6250-5125

References

[1] R. Damadian, Science **171**, 1151 (1971).
[2] I. C. Kiricuta and V. Simplceanu, Cancer Res. **35**, 1164 (1975).
[3] E. Belorizky, P.H. Fries, L. Helm, J. Kowalewski, D. Kruk, and P.O. Westlund, J. Chem. Phys. **128**, 052315 (2008).
[4] J. Kowalewski, D. Kruk, and G. Parigi, Adv. Inorg. Chem. **57**, 41 (2005).
[5] P. Caravan, Chem. Soc. Rev. **35**, 512 (2006).
[6] P. Caravan, J.J. Ellison, T.J. McMurry, and R.B. Lauffer, Chem. Rev. **99**, 2293 (1999).
[7] T. Nilsson and J. Kowalewski, J. Magn. Reson. **146**, 345 (2000).
[8] I. Bertini, C. Luchinat, and G. Parigi, *Solution NMR of Paramagnetic Molecules* (Elsevier, Amsterdam, 2001).
[9] D. Kruk, T. Nilsson, and J. Kowalewski, Phys. Chem. Chem. Phys. **3**, 4907 (2001).
[10] D. Kruk and J. Kowalewski, Mol. Phys. **101**, 2861 (2003).
[11] I. Bertini, O. Galas, C. Luchinat, and G. Parigi, J. Magn. Reson. **113**, 151 (1995).
[12] T. Nilsson, J. Svoboda, P.-O. Westlund, and J. Kowalewski, J. Chem. Phys. **109**, 6364 (1998).
[13] D. Kruk, T. Nilsson, and J. Kowalewski, Mol. Phys. **99**, 1435 (2001).
[14] D. Kruk and J. Kowalewski, Mol. Phys. **101**, 2861 (2003).
[15] C. Gösweiner, P. Lantto, R. Fischer, C. Sampl, E. Umut, P-O. Westlund, D. Kruk, M. Bödenler, S. Spirk, A. Petrovič, and H. Scharfetter, Phys. Rev. X **8**, 021076 (2018).
[16] D. Kruk, E. Umut, E. Masiewicz, C. Sampl, R. Fischer, S. Spirk, C. Gösweiner, and H. Scharfetter, Phys. Chem. Chem. Phys. 20, 12710 (2018).
[17] D. Kruk, A. Kubica, W. Masierak, A. F. Privalov, M. Wojciechowski, and W. Medycki, Solid State Nucl. Magn. Reson. **40**, 114 (2011).
[18] P.-O. Westlund, Mol. Phys. **107**, 2141 (2009).
[19] P.-O. Westlund, Phys. Chem. Chem. Phys. **12**, 3136 (2010).
[20] F. Winter and R. Kimmich, Mol. Phys. **45**, 33 (1982).
[21] F. Winter and R. Kimmich, Biophys. J. **48**, 331 (1985).
[22] E. Anoardo and D.J. Pusiol, Phys. Rev. Lett. **76**, 3983 (1996).
[23] D.J. Lurie, S. Aime, S. Baroni, N.A. Booth, L. M. Broche, C.-H. Choi, G.R. Davies, S. Ismail, D. Ó hÓgáin, and K.J. Pine, Comptes Rendus Phys. **11**, 136 (2010).
[24] L.M. Broche, G.P. Ashcroft, and D.J. Lurie, Magn. Reson. Med. **68**, 358 (2012).
[25] L.M. Broche, S.R. Ismail, N.A. Booth, and D.J. Lurie, Magn. Reson. Med. **67**, 1453 (2012).
[26] M. Bödenler, M. Basini, M.F. Casula, E. Umut, C. Gösweiner, A. Petrovic, D. Kruk, and H. Scharfetter, J. Magn. Reson. **290**, 68 (2018).
[27] M. Florek-Wojciechowska, R. Jakubas, and D. Kruk, Phys. Chem. Chem. Phys. **19**, 11197 (2017).
[28] D. Kruk and O. Lips, J. Magn. Reson. **179**, 250 (2006).
[29] D. Kruk, J. Altmann, F. Fujara, A. Gadke, M. Nolte, and A.F. Privalov, J. Phys. Condens. Matter **17**, 519 (2005).
[30] D. Kruk, A. Kubica, W. Masierak, A.F. Privalov, M. Wojciechowski, W. Medycki, Solid State Nucl. Magn. Reson. **40**, 114 (2011).
[31] D. Kruk, A. Privalov, W. Medycki, C. Uniszkiewicz, W. Masierak, and R. Jakubas, Annual Reports on NMR Spectroscopy 76, (2012), p. 67.
[32] D. Kruk, *Understanding Spin Dynamics* (Pan Stanford Publishing Pte Ltd, Singapore, 2015).
[33] A. Abragam, *The Principles of Nuclear Magnetism* (Oxford University Press, Oxford, 1961).

[34] C. Slichter, *Principles of Magnetic Resonance* (Springer-Verlag, Berlin, 1990).

[35] J. Kowalewski, A. Egorov, D. Kruk, A. Laaksonen, S.N. Aski, G. Parigi, and P.-O. Westlund, J. Magn. Reson. **195**, 103 (2008).

[36] R. Delgado and J.J.R.F. da Silva, Talanta **29**, 815 (1982).

[37] X. Sun, M. Wuest, Z. Kovacs, A.D. Sherry, R. Motekaitis, Z. Wang, A.E. Martell, M. J. Welch, and C. J. Anderson, J. Biol. Inorg. Chem. **8**, 217 (2003).

[38] K.D. Demadis, E. Barouda, N. Stavgianoudaki, and H. Zhao, Cryst. Growth Des. **9**, 1250 (2009).

[39] D.A. Moore, Org. Synth. **85**, 10 (2008).

[40] É. Csajbók, Z. Baranyai, I. Bányai, E. Brücher, R. Király, A. Müller-Fahrnow, J. Platzek, B. Radüchel, and M. Schäfer, Inorg. Chem. **42**, 2342 (2003).

[41] S. Hassfjell, K.O. Kongshaug, and C. Rømming, Dalton Trans. **0**, 1433 (2003).

[42] S. Aime, M. Botta, S.G. Crich, G. Giovenzana, R. Pagliarin, M. Sisti, and E. Terreno, Magn. Reson. Chem. **36**, S200 (1998).

[43] D. H. Powell, O.M. Ni Dhubhghaill, D. Pubanz, L. Helm, Y.S. Lebedev, W. Schlaepfer, and A.E. Merbach, J. Am. Chem. Soc. **118**, 9333 (1996).